Biochimica et Biophysica Acta, 972 (1988) 265–276
Elsevier

BBA 12362

Human platelet electrorotation change induced by activation: inducer specificity and correlation to serotonin release

Marcel Egger [a], Edwin Donath [a], Peter Spangenberg [b], Martina Bimmler [c], Roland Glaser [a] and Uwe Till [b]

[a] *Sektion Biologie, Bereich Biophysik, Humboldt-Universität zu Berlin, Berlin,* [b] *Medizinische Akademie Erfurt, Bereich Pathobiochemie, Erfurt and* [c] *Pathologisches Institut der Humboldt-Universität zu Berlin, Abteilung Ultrastrukturelle Pathologie und Elektronenmikroskopie der Charité, Berlin (G.D.R.)*

(Received 12 April 1988)
(Revised manuscript received 29 August 1988)

Key words: Electrorotation; Platelet activation; Membrane conductivity; Serotonin release; (Human)

Electrorotation of single platelets was compared with [^{14}C]serotonin release, aggregation and electron microscopy. Activation of washed and degranulated platelets was induced by thrombin, arachidonic acid, collagen, adrenaline, platelet activation factor (PAF), ADP and A23187. A strong correlation between electrorotation decrease and serotonin release was found. Electrorotation did not correlate with aggregation. It was concluded that an increase of the specific conductivity of the platelet membrane by three orders of magnitude (approx. $1.0 \cdot 10^{-7}$ S·m^{-1} to $1.0 \cdot 10^{-4}$ S·m^{-1}) upon activation was responsible for the observed decrease of anti-field rotation and the shift of the first characteristic frequency towards higher values. Electrorotation allowed for time-dependent measurements of activation. Characteristic activation times in the order of minutes were found. There was the following sequence of activators classified by increasing activation time constants: A23187 was the fastest followed by thrombin, collagen, PAF, arachidonic acid, adrenaline, and ADP.

Introduction

There are only a few biophysical methods available to investigate the activation behavior of single platelets. Of special interest is the study of membrane events at the single cell level during platelet activation. An earlier work [1] demonstrated that there were electrorotation changes during platelet activation. These rotation changes were interpreted to be caused by membrane conductivity changes during activation. As yet it has not been shown whether there is a general correlation between electrorotation and release or aggregation. In the earlier work only correlation between rotation and aggregation was found with one particular activator.

Electrorotation is a special dielectric spectroscopy technique which already has a number of successful applications [2–6]. Its advantage is that it can be applied to a single microscopic particle. The common dielectric spectroscopy technique of measuring the impedance of a suspension requires, in contrast, relatively high particle concentrations. The other method, dielectrophoresis, is extremely difficult to perform quantitatively.

It is well known that almost all biological objects observe several ranges of dispersion as a function of frequency of the external electric field

Correspondence: M. Egger, Sektion Biologie, Bereich Biophysik, Invalidenstrasse 42, Berlin 1040, G.D.R.

[7]. These dispersion ranges can be attributed to different mechanisms and are of different intensity. While all other dielectric spectroscopy methods finally detect the total complex dielectric constant, it is only electrorotation which is specifically sensitive to dispersion. Therefore, dispersion spectra can be obtained immediately by means of electrorotation. These spectra contain all information about the dielectric properties of the particle [8]. The reason for immediately obtaining dispersion spectra is that, only if dispersion is present, the vector of polarization and the external field vector form an angle which results in a torque applied to the particle. The speed of rotation is a measure of that specific part of the total dipole moment showing dispersion. The maximum rotation speed occurs just in the middle of the dispersion range (characteristic frequency). The direction of rotation gives additional information about the mechanism of the particular dispersion.

For none of the methods of dielectric spectroscopy is a theory for inhomogeneous nonspherical particles available. Despite that, these techniques are widely used in biology and colloid chemistry [9,10]. The available electrorotation theory describes the case of symmetrical particles only [11–13]. This theory shows that the conductance properties are extremely important for dispersion. In the case of cells there are usually two dispersion ranges in the kHz and MHz range. The first dispersion is due to the fact that the membrane has much lower conductivity than exterior and interior solution. This creates polarization of the particle caused by ionic clouds in front of and behind the particle (Maxwell-Wagner polarization) if an external electric field is applied. At higher frequencies of the external field applied, the membrane becomes shortcircuited by its capacity, leading to a possible conductivity difference between intracellular and external solution which is responsible for the resulting polarization. So, electrorotation may provide information about membrane and internal conductivity of a single particle.

The main result of our earlier work was that in the first dispersion range electrorotation decreased strongly when platelets were activated [1]. The only explanation of this behavior was that the conductivity of the plasma membrane of platelets increased. The high frequency dispersion range (co-field rotation range) was not investigated. Now, a better technique has allowed for investigation of the internal conductivity behavior during platelet activation too.

Release is due to exocytosis which is a result of granule membrane fusion. The cause and significance of the above discussed conductivity changes during activation observed for the first time in our earlier work are completely unknown. It was not clear whether this possible conductivity change reflected a distinct step within the exocytotic release reaction sequence. One may speculate that it might be related to the mechanism or be a result of the fusion process, because ionic permeability changes are believed to be of significance in regulating, initiating or completing exocytosis [14–17].

Of course, ionic permeability is closely related to conductivity and, therefore, electrorotation is a suitable method to study transient permeability changes.

To gain further insight into the mechanism on how the membrane and internal conductivity might change during activation it would be useful to study electrorotation during activation under more defined conditions. For example, it seemed promising to compare receptor- and ionophore-mediated activation to follow the release behavior in more detail. We had also not yet shown whether there was a correlation between release and electrorotation change, since in no case does the extent of release occur in parallel with the aggregation change.

Material and Methods

Blood collection and serotonin loading

Blood was withdrawn by vein puncture from healthy donors who had taken no drugs during the previous 2 weeks.

Immediately after vein puncture the blood was mixed with 0.1 vol. of 3.12% (w/v) sodium citrate (pH 7.4). Platelet-rich plasma was prepared by centrifugation at $200 \times g$ for 15 min at room temperature. The supernatant platelet-rich plasma was incubated with 1 μM 5-hydroxy[*side chain*-2-^{14}C]tryptamine creatinine sulfate ([^{14}C]serotonin, spec. 55 mCi/mmol, CFA 170, The Radiochemical Centre, Amersham, U.K.) for 30 min at 37 °C,

in order to label the serotonin-dense granules.

The labeled platelet-rich plasma was stored in closed plastic tubes at 37°C. Measurement of serotonin release was performed according to Heptinstall et al. [18].

Platelet degranulation

After centrifugation of platelet-rich plasma ($300 \times g$, 15 min, room temperature), the supernatant was discarded. Platelets were washed twice to remove plasma constituents ($300 \times g$, 15 min, at room temperature) and resuspended in a washing buffer of the following composition: 36 mM citric acid, 5 mM glucose, 5 mM KCl, 90 mM NaCl, 1 μM prostaglandin E_1 (PGE_1, P-5515, Sigma), 10 mM EDTA-Na salt. pH of the washing buffer was adjusted to 6.5 with conc. NaOH.

The pellet was resuspended into Hepes-Tyrode buffer (5.55 mM glucose, 5.45 mM NaH_2PO_4, 0.01 mM $MgCl_2$) adjusted to pH 7.35. Subsequently, the radioactivity of the washed platelet suspension and the supernatant was measured. The suspension of washed platelets was divided into two equal parts and kept at 37°C. One part was degranulated using a modified method of Kinlough-Rathbone et al. [19] and the other was used to determine the control values of aggregation and electrorotation.

Degranulation was performed by incubating washed platelets with 0.5 U/ml thrombin (Arzneimittelwerk Dresden, G.D.R.) for 10 min at 37°C without stirring. The process was stopped by adding ACD solution (38 mM citric acid, 74.8 mM sodium-citrate, 134.8 mM glucose). The radioactivity of both the ACD suspension and the supernatant was measured to determine the [^{14}C]serotonin release count.

Aggregation

Platelet aggregation was induced by 4 μg/ml collagen (Collagenreagent Horm, München, F.R.G.), 0.5 U/ml thrombin or 0.1 μM A23187 (Sigma) at 37°C. The aggregation traces were monitored with a dual channel aggregometer (ELVI 80, Elvi Logos, Milan, Italy).

Measurement of platelet release reaction

In order to compare different inducers with regard to their potential for inducing release it was necessary to calibrate the platelet-rich plasma system on an equal aggregation trace for each blood sample. Beginning with an activator concentration sufficient for maximum aggregation, it was decreased step by step to find for each inducer with each sample a concentration yielding the same degree of biphasic aggregation. This is shown for ADP and PAF in Fig. 1. For different blood samples different concentrations of each activator were necessary. The following inducers and concentration ranges were employed: 0.1–1.0 U/ml thrombin, 0.312–1.5 μM ADP (Reanal, Budapest, Hungary), 3.12–10 μM adrenaline (AdW Berlin, G.D.R.), 0.5–2.0 mM arachidonic acid (Sigma), 1.0–4.0 μg/ml collagen, 1.5–5.0 μM PAF (1-*O*-alkyl-2-acetyl-*sn*-glycero-3-phosphocholine, semisynthetic PAF-acether, Prof. H.K. Mangoldt, Münster, F.R.G.), 0.02–0.15 μM A23187. [^{14}C]Serotonin-loaded platelet-rich plasma was used.

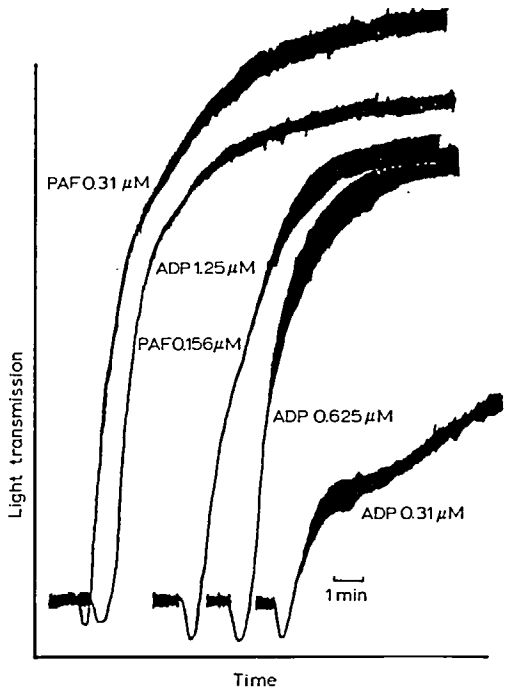

Fig. 1. Example of calibration on equal aggregation traces. Maximum aggregation induced by 0.31 μM PAF, 1.25 μM ADP and a different degree of biphasic aggregation induced by 0.31 μM ADP; concentration for inducer investigations were 0.156 μM PAF and 0.625 μM ADP. For the concentrations of other inducers see Table I.

Electrorotation

Platelets were resuspended into the measuring solution (300 mosM sucrose, 5.8 mM phosphate-buffered saline (PBS) buffered at pH 7.2) yielding a final cell density of 50–200 platelets per μl. This was performed by adding 2 μl of platelets to 1 ml rotation solution. The suspension was kept at 37° C.

The suspension conductivity was determined before and after rotation measurements with a conductometer (LM 301 Hydromat, G.D.R.) at 22° C. Conductivities of $0.19 \pm 0.1 \cdot 10^{-3}$ S · m^{-1} were achieved. The temperature in the measuring chamber was 22° C. Cell dimensions and electrorotation were recorded with a microscope (JENAVAL, Carl-Zeiss, Jena, G.D.R.) fitted with phase contrast optics (objective: HI 100°/1.25, ocular: GF-PW 10×). A 1.45 mm^2 measuring chamber described earlier [1] (1.26 μl volume) was used. One-line computer control of frequency and data evaluation allowed the measurement of a whole frequency spectrum to be performed within 60 s. The electrical equipment consisted of a TV-camera and monitor, a newly developed digital rotation-field-generator (RFG-5, Humboldt-University Berlin, Division of Biophysics, G.D.R. [20,21]), a frequency counter (G-2002.500, RFT, Erfurt, G.D.R.), amplifier (RFG-5E, Humboldt-University Berlin, Division of Biophysics, G.D.R.) and a microcomputer system (Commodore).

Transmission electron microscopy

Degranulated platelets were fixed for 30 min in 2.5% glutaraldehyde (Serva) at room temperature. After centrifugation at 10000 × g for 10 min at 22° C the pellet was transferred into Hepes-Tyrode

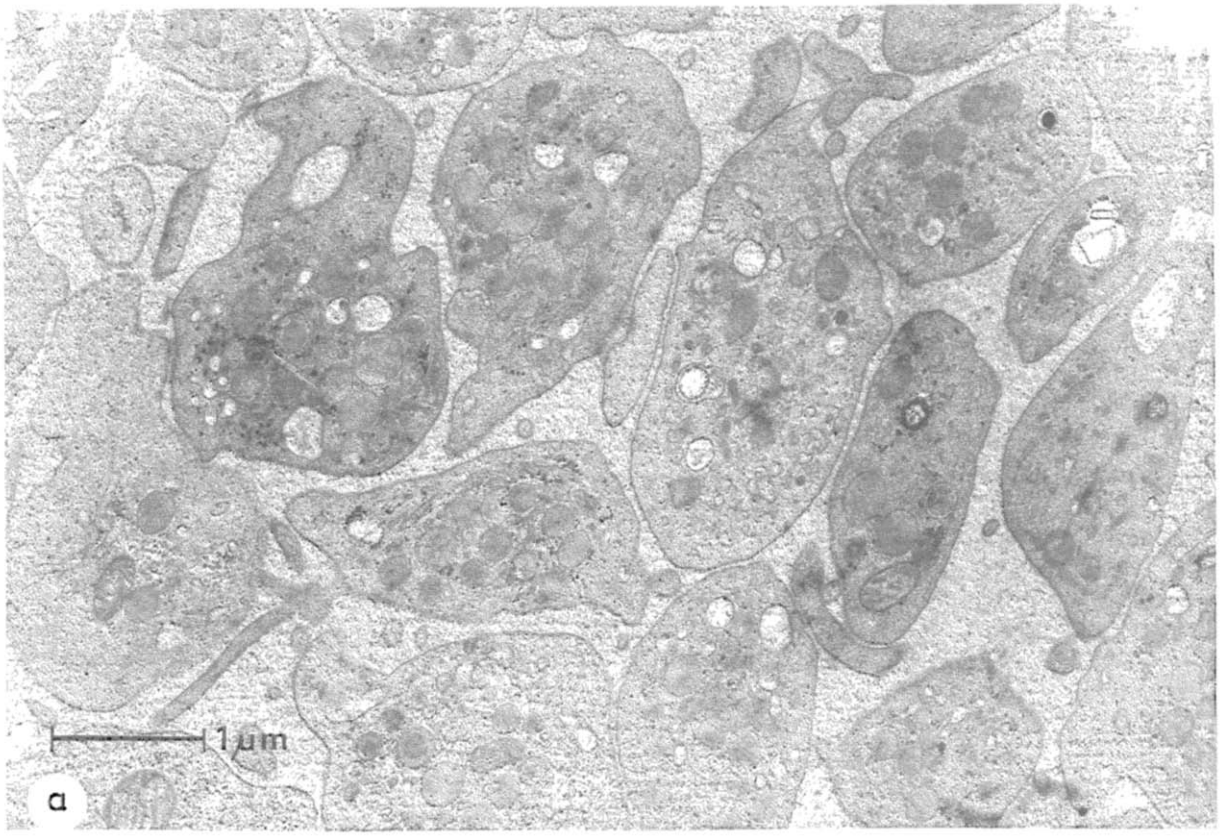

Fig. 2. Transmission electron micrograph of (a) control (×20000) and (b) degranulated platelets (×10000). Platelets were degranulated with 0.5 U/ml thrombin for 10 min at 37° C. Platelets were incubated in Hepes-Tyrode buffer without stirring. Note the highly irregular platelet circumference, the disappearance of α-granules and the large vacuolar structure of degranulated platelets.

buffer. A transmission electron microscope was used and magnifications of 10000 and 20000 were made.

Results

Electrorotation of degranulated platelets

Since the activation process of platelets is a complex sequence of events in terms of both membrane organization and biochemistry it was very difficult to relate the earlier observed electrorotation change to particular steps within the activation cascade. Therefore we prepared degranulated platelets. In these platelets certain steps of the activation process had taken place. Due to addition of prostaglandin and manipulation of pH, activation could be arrested at an advanced level where only serotonin release had been mostly completed. By means of electron microscopy, [^{14}C]serotonin release analysis and measurements of the aggregation potency it was possible to characterize the platelet condition quite precisely. The advantage of this preparative method was to investigate platelets independently of time effects.

Fig. 2a and b proves that activation and degranulation had been achieved to a certain extent. Control platelets were compared with degranulated platelets. During thrombin-induced degranulation the discoid shape of non-activated platelets transformed into a completely irregulator one (Fig. 2a and b). Especially remarkable was the formation of pseudopods and loop-like structures. The overall surface-connected canalicular system (SCCS) seemed to be swollen and widened. The electron-dense granules were replaced by vacuoles indicating that fusion processes had taken place during the exocytotic release reaction between serotonin-containing granules, the SCCS and the outer platelet membrane. Cut off parts of membrane material were found in the platelet vicinity.

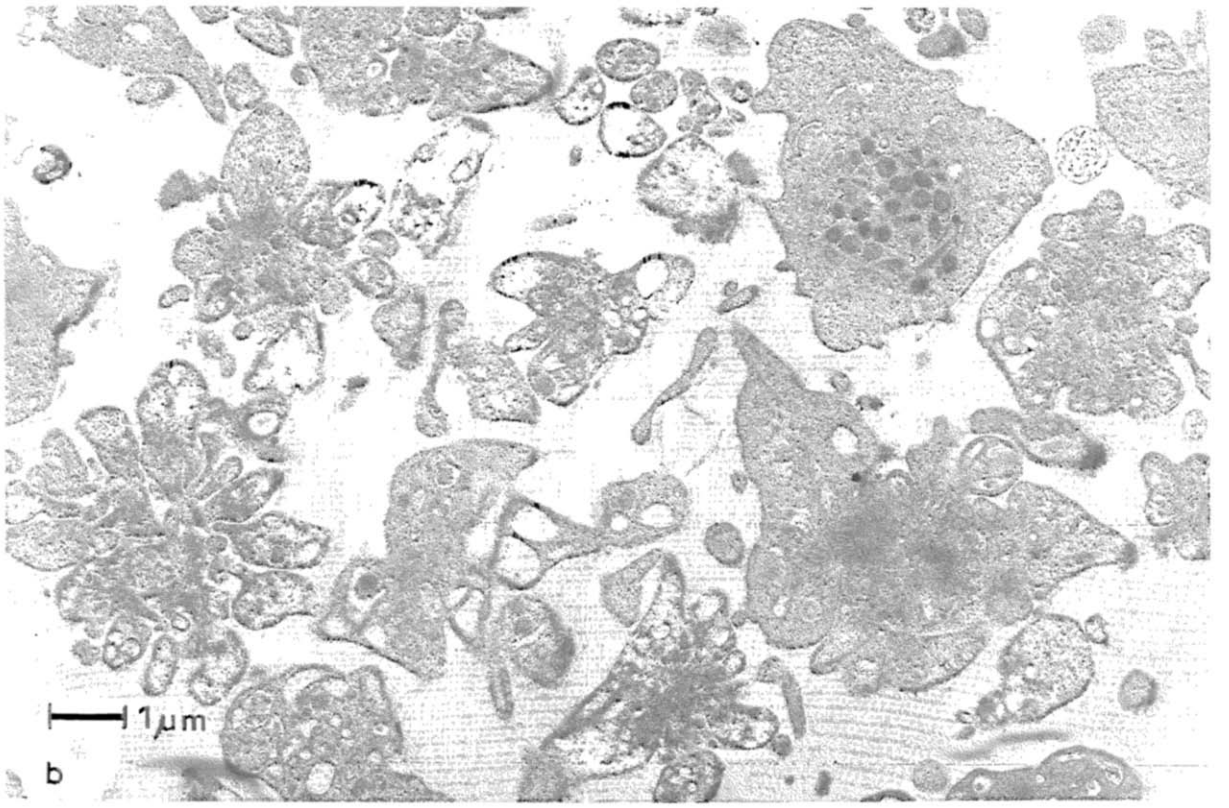

Fig. 2 (continued).

Platelets can give off lipid-rich material known as 'platelet dust' or 'microparticles' [22]. A significant increase of the platelet radius by about 1/3 was ascertained for platelets with high granule-releasing rates. It was also obvious that degranulated platelets did not represent a homogeneous population, as Fig. 2a clearly shows. Platelets with an apparently complete amount of their granules were found together with completely activated platelets, but a contraction in the cytoskeletal system and a concentration of granules in an electron-dense zone within apparently granule-containing platelets indicated that the activation process had been induced, at least partially.

Different degranulation experiments yielding different release rates ranging from 60 to 90% serotonin release which were donor-dependent provided us with the possibility to compare release rates of degranulated platelets with electrorotation.

The population of degranulated platelets showed a relatively inhomogeneous electrorotation behavior in the anti-field rotation range. While one portion of platelets rotated other platelets did not show rotation. Now, for each sample the [^{14}C]serotonin release was measured and compared with the number of platelets without anti-field rotation. In Fig. 3 a correlation between the increase of platelets with non-measurable rotation in the first characteristic frequency range and the [^{14}C]serotonin release was observed. At a release level of 60% only 20% of the platelets showed no rotation. Release values under 60% hardly influenced the number of platelets without anti-field rotation. Nearly all platelets rotated but of course more slowly than the control, as was obvious from Fig. 3. If the release value reached a percentage above 60% the number of platelets without anti-field rotation increased very rapidly. So, at 90% [^{14}C]serotonin release only few platelets rotated. An analysis of the electrorotation properties of the degranulated platelets which still rotated showed that in the anti-field rotation range the first characteristic frequency of the degranulated platelets was shifted by approximately 20% towards higher frequencies (Fig. 4) as compared with the control. In parallel, a decrease of the anti-field rotation by about 1/3 occurred. Subsequent stimulation with thrombin induced a further

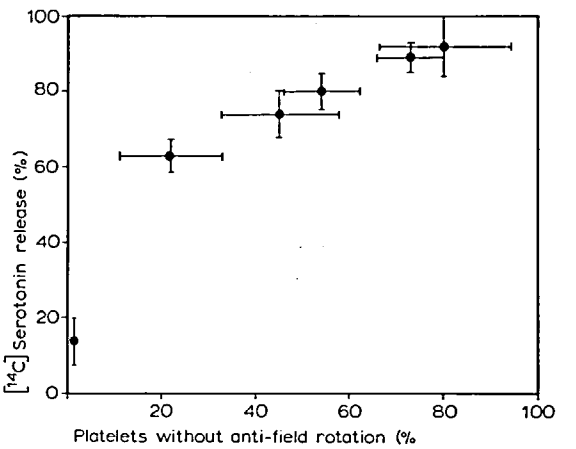

Fig. 3. Percentage of degranulated platelets not rotating in the first characteristic frequency range as a function of [^{14}C]serotonin release during degranulation. Rotation measurements at 0.32, 0.56 and 1.0 MHz, 300 mosM sucrose, 5.8 mM PBS, pH 7.2. The filled circle in the left-hand lower corner represents the control.

shift of the first characteristic frequency by about 17% towards higher frequencies as compared with degranulated platelets. The anti-field rotation decreased further too. The second characteristic frequency and the co-field rotation, however, did not change significantly.

Inducer specificity of electrorotation

In an earlier work we observed a decrease of electrorotation as a function of time in the first characteristic frequency range after thrombin-induced activation [1]. The half-time of this decrease corresponded to the half-maximum aggregation.

It is well known that agonists like thrombin, arachidonic acid, ADP, collagen, PAF, adrenaline or the ionophore A23187 (Table I) differ in their potential to induce the serotonin release reaction [22–24]. Consequently, from the results of the experiments with degranulated platelets one may expect different sensitivities of electrorotation upon activation.

Since at the same time there were donor-dependent differences in the release and aggregation as well as differences in sensitivity towards the same agonist, it followed that for comparison the platelet system had to be calibrated. One example was given in Fig. 1.

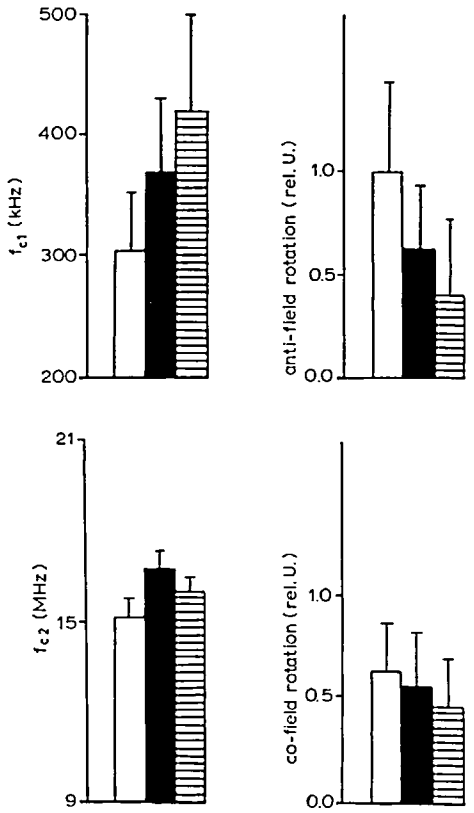

Fig. 4. First characteristic frequency (f_{c1}), anti-field rotation and second characteristic frequency (f_{c2}), co-field rotation of washed platelets (open bars), degranulated platelets (filled bars), and degranulated platelets activated with 1.0 U/ml thrombin, 5 min (hatched bars). The rotation was divided by the maximum rotation of control. 300 mosM sucrose/5.8 mM PBS (pH 7.2), $n = 26$, S.E.

TABLE I

^{14}C]SEROTONIN RELEASE IN THE PLATELET-RICH PLASMA SYSTEM CALIBRATED ON EQUAL AGGREGATION TRACES

Different blood samples, $n = 12$, ±S.E. The wide concentration ranges resulted from donor-dependent differences (see Materials and Methods).

nducer	Concentration	[^{14}C]Serotonin release
A23187	0.025–0.1 μM	90.0± 8.3
Thrombin	0.25±1.0 U/ml	82.7± 7.2
Collagen	1.0–2.5 μg/ml	63.1±11.0
PAF	0.031–0.156 μM	50.5±10.3
ADP	0.312–1.25 μM	38.8± 6.6
Arachidonic acid	0.5–2.5 mM	30.8±10.6
Adrenaline	7.5–10.0 μM	25.1± 6.8

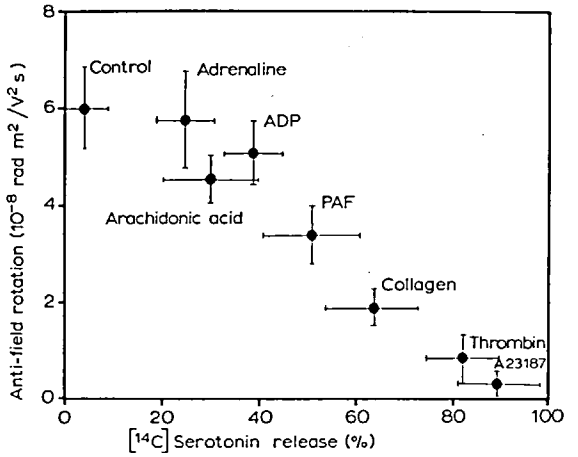

Fig. 5. Anti-field rotation as a function of [^{14}C]serotonin release. Concentrations of inducers according to Table I calibrated on equal aggregation traces.

In Fig. 5 we compared the [^{14}C]serotonin release and anti-field rotation of adrenaline-, arachidonic acid-, ADP-, thrombin-, collagen-, PAF- and Ca^{2+}-ionophore A23187-activated platelets obtained 5 min after application of the activator. It was obvious that the efficiency of the individual activators with respect to serotonin release correlated with the rotation change in the range of anti-field rotation if the release was at least 40%. The more efficient the release reaction of the particular inducer, the larger the decrease of the anti-field rotation (Fig. 5). This was typical for the Ca^{2+}-ionophore A23187, thrombin, collagen

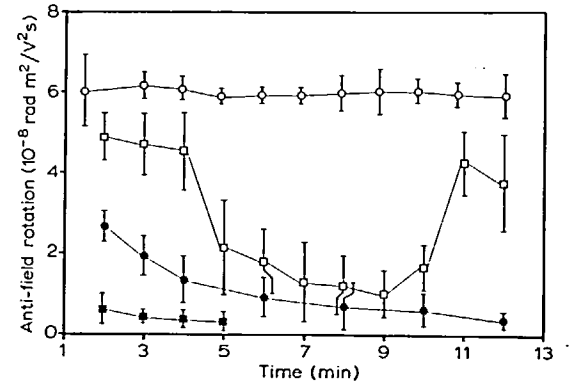

Fig. 6. Anti-field rotation of activated platelets as a function of time. ○, control; □, collagen; ●, thrombin; ■, A23187. 300 mosM sucrose, pH 7.4, 5.8 mM PBS. Rotation was measured at 560 kHz. Inducer concentrations are given in Table I.

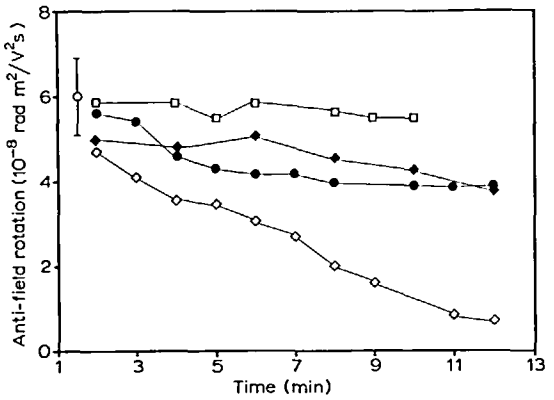

Fig. 7. Anti-field rotation of activated platelets as a function of time. □, adrenaline; ■, PAF; ◆, ADP; ◇, arachidonic acid. 300 mosM sucrose, 5.8 mM PBS, pH 7.4. Rotation was measured at 560 kHz. Inducer concentrations are given in Table I.

and PAF (semi-synthetic PAF-acether). Weak inducers with a release potency of less than 40% [^{14}C]serotonin release did not show a correlation between the decrease of the anti-field rotation and [^{14}C]serotonin release.

It must be emphasized that despite calibration on equal aggregation traces individual activators induced different electrorotation kinetics (Figs. 6 and 7) and also different [^{14}C]serotonin release reactions. In addition, under our activation conditions there were differences in the degree of homogeneity of the electrorotation behavior of the total platelet population.

Kinetics of electrorotation change

Now we were interested in finding out whether the kinetics of the electrorotation change induced by different activators showed specificity in the first characteristic frequency range.

The Ca^{2+} ionophore A23187 produced the fastest decrease in electrorotation (Fig. 6). Already after 2–3 min of incubation the rotation decreased to about 1/10 of the original value. This agreed with the increase in the number of platelets without rotation within the overall population. After 2–3 min only 40% of the platelets still rotated. After 5 min the process of rotation decrease was complete and about 90% of the platelets showed no rotation. In the case of thrombin activation, after 7 min two opposite developments in the process of rotation changes were observed. Whereas one portion of platelets showed a further decrease in rotation another again started to rotate. This behavior is not reflected in the graph (Fig. 6). On average 40–50% of the platelets rotated with 25% of the initial rotation value in the case of thrombin activation.

The rotation increase after a period of drastic decrease was even more clearly pronounced following collagen activation. After 10 min most platelets rotated with their initial rotation value. Only thrombin and collagen showed inhomogeneous rotation behavior. Ionophore A23187, PAF, ADP and arachidonic acid activation reactions were in general more homogeneous (Fig. 7). With the latter agonists dramatic decreases of the anti-field rotation to unmeasurably small values did not occur within the observed period of time. Strong inducers, however, caused a maximum decrease in anti-field rotation during the first 2 min. In the case of poor release inducers an almost linear course of rotation decrease as a function of time was found.

Discussion

The results of inducer investigations together with the electrorotation behavior of degranulated platelets demonstrated clearly a correlation between release and decrease of rotation in the range of the first characteristic frequency (Figs. 3 and 5). Since, for example, in Fig. 5 all activators induced the same aggregation it was also clear that the electrorotation decrease did not necessarily correlate with aggregation. These new results supported the hypothesis of our previous studies on thrombin activation that electrorotation could be used to obtain a new valuable activation parameter of an individual platelet [1]. In order to understand and to interpret the results of electrorotation measurements we employed in this study standard methods for investigating platelet functions, e.g., measurement of [^{14}C]serotonin release, electron microscopy and aggregation.

Theoretical remarks

A comprehensive theoretical interpretation of electrorotation behavior of single and multi-shell models is available on the basis of the work of Zimmermann, Fuhr and Sauer [5,25,26]. Since our

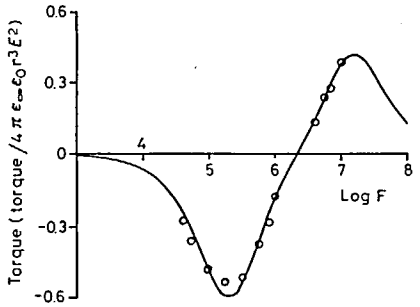

Fig. 8. Torque of a single washed non-activated platelet as a function of frequency of the applied electric field. 300 mosM sucrose/5.8 mM PBS (pH 7.2). The solid line is a theoretical curve of the dimensionless torque (torque/$4\pi\varepsilon_\infty\varepsilon_0 r^3E^2$) according to the single-shell model [1] with the following parameters: radius = 1.1 μm, membrane thickness = $8\cdot10^{-8}$ m, dielectric constant of bulk solution = 80, membrane dielectric constant = 7.2, dielectric constant of platelet interior = 50, bulk solution specific conductivity = $0.68\cdot10^{-3}$ S·m^{-1}, specific conductivity of platelet interior = 0.16 S·m^{-1}, membrane specific conductivity = $1.0\cdot10^{-7}$ S·m^{-1}. The measured data were multiplied by an empirical factor in order to bring the peak heights into coincidence with the theoretical fit. This was necessary because neither the friction nor the field strength are known precisely enough.

measured data were similar to the theoretically predicted behavior of the single-shell model the latter was used for the interpretation of the measurements (Fig. 8).

Despite the very complex morphology of platelets they surprisingly showed nevertheless a simple electrorotation behavior. In resting platelets we found different shapes (Fig. 6a), such as ellipsoidal, often with very irregular membrane invaginations which increase the extent to which the membrane surface is accessible from the outside, and populations of granules with different sizes. The rotation behavior of biological particles in an externally applied rotating electric field in the range of anti-field rotation depends mainly on the cell radius (r), the membrane dielectric constant (ε_m) and the membrane conductivity (G_m) as well as on the internal conductivity (G_1) [2,3,5,11–13]. Of course, the shape should also influence the electrorotation behavior, because it determines the value of the dipole moment and hydrodynamic friction. Although a theoretical analysis of electrorotation for nonspherical particles is not available it was clear from the general polarization properties that nonsphericity and irregularity cannot qualitatively influence the electrorotation behavior. Nonsphericity as well as problems in determining the field strength at the position of the particle at present did not allow a quantitative comparison of the rotation measured with its theoretical value. Only the frequency dependence and the relative peak heights can be used for interpretation of experimental data. From the analysis of the multi-shell models we also know that internal structures such as vesicles hardly influence the electrorotation behavior in the range of the first characteristic frequency [27].

Explanation of the decrease of electrorotation upon activation

The most significant result of the electrorotation experiments was that electrorotation in the range of the first characteristic frequency decreased very strongly upon activation but was unaffected in the second characteristic frequency range. How can this behavior be explained?

Although we are aware of the fact that the single-shell model [7] cannot explain all details of the electrorotation behavior of platelets it should describe the general features of electrorotation of platelets correctly. By applying the single-shell model of Fuhr and Glaser [5,11–13] and by varying r, G_m, ε_m, and the internal conductivity (G_1) the influence of these parameters on the first characteristic frequency and the anti-field rotation was estimated (Fig. 9). We took as a reference the average anti-field rotation of washed control platelets at the first characteristic frequency. From the dependence of the rotation on frequency we estimated the parameters of these control cells [1]. Then we varied each parameter separately keeping other parameters constant. We then used this diagram to interpret the observed changes in electrorotation. The dramatic decrease of the anti-field rotation could only be explained by assuming an increase of the membrane conductivity (G_m). By increasing G_m from 10^{-7} S·m^{-1} to 10^{-4} S·m^{-1} the rotation can drop to 1/6 of its initial value. In parallel, the first characteristic frequency was shifted to higher frequencies. The transmission electron microscopic investigations suggested an increase of the effective radius by 20–35% after activation. This would result in a shift of f_{c1} to 11–23.5% lower frequencies without appreciably

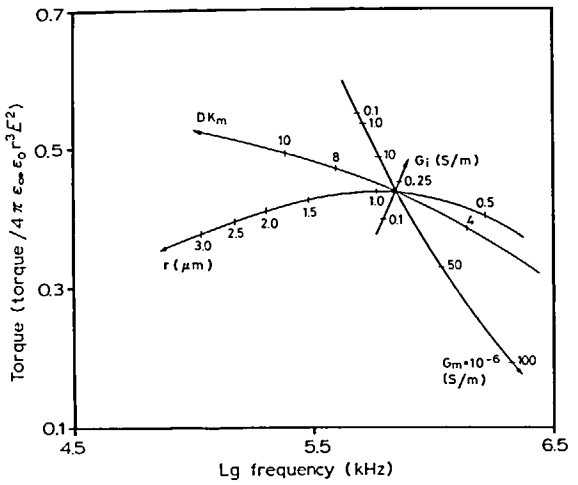

Fig. 9. Torque and frequency of the first peak of electrorotation calculated by means of the single-shell model [1]. The torque was divided by $4\pi\varepsilon_\infty\varepsilon_0 r^3E^2$, r being the radius and E the electric field strength. Starting values for variation were radius = $5\cdot10^{-7}$ m, membrane specific conductivity = $2.0\cdot10^{-5}$ S·m^{-1}, membrane dielectric constant = 5.7 and specific conductivity of platelet interior = 0.2 S·m^{-1}. They were each varied separately. The other parameters were kept constant: membrane thickness = $8\cdot10^{-9}$ m, dielectric constant of bulk solution (ε_∞) = 80, dielectric constant of platelet interior = 50, bulk solution specific conductivity = $6.7\cdot10^{-3}$ S·m^{-1}.

influencing the rotation value. Changes in the dielectric constant of the membrane also cannot explain the observed electrorotation changes upon activation.

Theoretical considerations [7] indicated that an increase of the surface charge density from $1.0\cdot10^{-2}$ cm^{-2} to $3.0\cdot10^{-2}$ cm^{-1} could decrease the torque in the first characteristic frequency range by about 30%. This is comparable to the maximum change in charge density possible in biological objects. However, during platelet activation the electrophoretic mobility decreased [28]. So it is obvious that the surface charge effect also cannot account for the observed rotation decrease.

Summarizing, we concluded that it can only be an increase of membrane conductivity which could be responsible for the decrease of electrorotation upon activation. On the other hand, the minor changes in the second characteristic frequency range indicated that the internal conductivity did not change significantly. So, one can infer that only either cations or anions were responsible for the increase of the membrane conductivity. Otherwise the platelets would have leaked out and the first characteristic frequency would have been shifted towards smaller values. As a consequence of or a prerequisite for the exocytotic release reaction the membrane conductivity attributed to this ionic species has to increase by at least orders of magnitude. A possible candidate could be Cl^-, since there is evidence that platelet activation was accompanied by an anion permeability increase [29].

This possible conductivity increase of the plasma membrane after activation could either be due to the incorporation of granule membranes or could be an increase of the original plasma membrane conductivity, or could be due to both processes.

According to the chemo-osmotic hypothesis of exocytosis [14,16,30–35], osmotic swelling is a prerequisite for the completion of the fusion process between vesicle and platelet membranes and for the release of content into the outer media to be accomplished [14,15]. However, osmotic swelling should be only possible if, at least transiently, the permeability of the vesicle membrane had increased. Our results are not in conflict with this hypothesis, because the observed membrane conductivity increase may well be connected to such a permeability increase.

Activation kinetics

Now, let us discuss in more detail the differences in the activation kinetics (Figs. 6 and 7). It was obvious that different inducers not only showed a different efficiency but also exhibited differences in the kinetic behavior of electrorotation. Release reaction kinetics ranging from 4 s to about 3 min [17] were determined by other methods. Our measured electrorotation kinetics corresponded well with these data.

The receptor-coupled exocytotic release reactions induced by different activators were not only characterized by their efficient rotation decrease but also by their fast kinetics. No qualitative differences existed between the electrorotation kinetics of ionophore- and receptor-coupled exocytotic release reactions. A dramatic decrease of the anti-field rotation within the first 2 min was observed applying inducers such as thrombin, collagen, and the Ca^{2+}-ionophore A23187 (Fig. 6).

As mentioned above these inducers initiated a strong serotonin release, too. In contrast, adrenaline or ADP had slow rotation decrease kinetics (Fig. 7). This could be a further hint supporting the existence of different exocytotic pathways [22,36]. Also differences in the sizes of the granule populations fusing and, possibly, differences in the fusion mechanisms have been reported. It has been shown that there is exocytosis like a 'slow-release pill'. A mechanism of exocytosis as proposed by Pollard et al. [14,15] also could be possible.

Quite interesting was the relaxation of the electrorotation decrease after thrombin activation and more evidently in the case of collagen activation (Fig. 6). A similar process of membrane recovery was found in adrenal medullary cells [37]. The recovery of the electrorotation value after several minutes can be explained by a decrease of the membrane conductivity approaching its original value. The fact that such a recovery was never found with the Ca^{2+}-ionophore A23187 showed that platelet functions were irreversibly disturbed by a continuous Ca^{2+}-shortcircuit. For this reason a possible exo-endocytosis cycle was interrupted. Such cycles have not been observed in platelets yet, but it may be possible by using immunocytochemical methods based on antibodies to special serotonin-granule membrane proteins which become exposed at the cell surface during exocytosis.

In summary, we would like to mention that electrorotation has been proved useful for studying activation events of platelets on the single particle level. Information about membrane conductivity changes as a function of time that is hardly available with other methods can be obtained. However, the complex morphology of platelets has not yet permitted a detailed quantitative interpretation of the rotation data represented.

Acknowledgements

We would like to thank Mrs. Cordula Wagner from the Department of Pathological Biochemistry, Medical Academy of Erfurt for expert technical assistance, Dr. Axel-M. Ladhoff from the Institute of Pathology and Electronmicroscopy of the Charité (Berlin) for the excellent electron microscopy and Dr. sc. G. Fuhr (Berlin) for helpful discussion.

References

1 Egger, M., Donath, E., Ziemer, S. and Glaser, R. (1986) Biochim. Biophys. Acta 861, 122–130.
2 Arnold, W.M., Geier, B.M., Wendt, B. and Zimmermann, U. (1987) Biochim. Biophys. Acta 330, 65–71.
3 Arnold, W.M., Wendt, B., Zimmermann, U. and Korenstein, R. (1985) Biochim. Biophys. Acta 813, 117–131.
4 Arnold, W.M. and Zimmermann, U. (1982) Naturwissenschaften 69, 297.
5 Fuhr, G., Glaser, R. and Hagedorn, R. (1986) Biophys. J. 49, 395–402.
6 Gimsa, J., Fuhr, G. and Glaser, R. (1985) Stud. Biophys. 109, 5–14.
7 Pethig, R. and Kell, D.B. (1987) Phys. Med. Biol. 32, 933–970.
8 Pastushenko, V.Ph., Kuzmin, P.I. and Chizmadzev, Yu.A. (1985) Stud. Biophys. 110, 51–57.
9 Kell, D.B. and Harris, Ch.M. (1985) J. Bioelectr. 4, 317–348.
10 Irimajiri, A., Asami, K., Ichinowatari, T. and Kinoshita, Y. (1987) Biochim. Biophys. Acta 986, 203–213.
11 Fuhr, G. (1985) Dissertation B, Humboldt-University, Berlin.
12 Glaser, R. and Fuhr, G. (1987) in Mechanistic Approaches to Interactions of Electric and Electromagnetic Fields with Living Systems (Blank, M. and Findl, E., eds.), pp. 271–290, Plenum Press, New York.
13 Glaser, R. and Fuhr, G. (1986) in Electric Double Layers in Biology (Blank, M., ed.), pp. 227–242, Plenum Press, New York.
14 Pollard, H.B., Tack-Goldmann, K., Pazoles, C.J., Creutz, C.E. and Shulman, N.R. (1977) Proc. Natl. Acad. Sci. USA 74, 5295–5299.
15 Pollard, H.B., Pazoles, C.J., Creutz, C.E. and Zinder, O. (1979) Int. Rev. Cytol. 58, 159–197.
16 Zimmerberg, J. and Whitaker, M. (1985) Nature 315, 581–584.
17 Zimmerberg, J., Sardet, C. and Epel, D. (1985) J. Cell Biol. 101, 2398–2410.
18 Heptinstall, S., Bevan, J., Cockbill, S.R., Hanley, S.P. and Parry, M.J. (1980) Thromb. Res. 20, 219–230.
19 Kinlough-Rathbone, R.L., Chahil, A., Packham, M.A., Reimers, H.-J. and Mustard, J.F. (1975) Thromb. Res. 7, 435–449.
20 Arnold, W.M. and Zimmermann, U. Patent Application, Official Designation P 3325 843.0 (recorded at the patent office, F.R.G.), 18 July, 1983.
21 Gimsa, J., Fuhr, G. and Glaser, R. Patent Application, Official Designation WP G01N/281223 (recorded at the patent office, G.D.R.) 1986.
22 Skear, R.J. (1981) in Platelets in Biology and Pathology, Vol. 2 (Gordon, J.L., ed.), pp. 321–348, Elsevier/North-Holland, Amsterdam.

23 Holmsen, H., Day, H.J. and Stormorken, H. (1969) Scand. J. Haematol. Suppl. 8, 3–28.
24 White, J.G. (1973) Ser. Haematol. 6, 49–98.
25 Arnold, W.M. and Zimmermann, U. (1982) Z. Naturforsch. 37c, 908–915.
26 Sauer, F.A. and Schlögel, R.W. (1985) in Interactions between Electromagnetic Fields and Cells (Chiabrera, A., Nicolini, C. and Schwan, H.P., eds.), pp. 203–225, Plenum Press, New York.
27 Fuhr, G., Geißler, F., Müller, T., Hagedorn, R. and Torner, H. (1987) Biochim. Biophys. Acta 930, 65–71.
28 Stoltz, J.F. (1983) Ann. N.Y. Acad. Sci. 416, 720–739.
29 Brown, E.M., Pazoles, C.J., Creutz, C.E., Aurbach, G.D. and Pollard, H.B. (1978) Proc. Natl. Acad. Sci. USA 75, 876–880.
30 Lucy, J.A. and Ahkong, Q.F. (1986) FEBS Lett. 199, 1–11.
31 Finkelstein, A. and Zimmerberg, J. (1986) Annu. Rev. Physiol. 48, 163–174.
32 Hampton, R.Y. and Holz, R.W. (1983) J. Cell Biol. 96, 1082–1088.
33 Zimmerberg, J. (1987) Biosci. Rep. 7, 251–269.
34 Holz, R.W. (1986) Annu. Rev. Physiol. 48, 175–189.
35 Zimmerberg, J., Curran, M., Cohen, F.S. and Brodwick, M. (1987) Proc. Natl. Acad. Sci. USA 84, 1585–1589.
36 Baker, P.F. and Knight, D.E. (1986) Br. Med. Bull. 42, 399–404.
37 Von Grafenstein, H., Roberts, C.S. and Baker, P.F. (1986) J. Cell Biol. 103, 2343–2352.